The chemical defense/offense in ciliated protists by means of toxic secondary metabolites

Federico Buonanno[1], Elisabetta Catalani[2], Davide Cervia[2], Gabriele Achille[1], Claudio Ortenzi[1]

[1] Laboratory of Protistology and Biology Education, Department of ECHT, Università di Macerata, 62100 Macerata, Italy
[2] Department for Innovation in Biological, Agro-food and Forest systems (DIBAF), Università della Tuscia, via S. Camillo de Lellis snc, 01100 Viterbo, Italy

INTRODUCTION

Several species of protists developed a number a different strategies intended to improve prey capture or avoid the predation. Particularly, in ciliated protist, the predator-prey interactions are often mediated by means some peculiar ejectable membrane-bound organelles generally called extrusomes. These organelles are usually localized in the cell cortex and attached to the cell membrane, sharing a common characteristic in discharging their contents to the outside of the cell in response to different stimuli (Fig. 1). Some of these extrusomes are known to function as defensive organelles as the cortical granules in *Climacostomum virens* (Fig. 2); others were demonstrated to have an offensive function (such as the toxicysts in raptorial ciliates, for example in *Colpes hirtus* (Fig. 3)), but the role of many other extrusomes remain unknown. Several of these extrusomes are known to produce toxic secondary metabolites that have been isolated from ciliates, and many of these molecules seem to be the result of evolutionary selection related to defense and/or predatory mechanisms. To date, only few of these molecules have been deep studied in function and biological activities, and include keronopsin isolated from *Pseudokeronopsis rubra*, euplotins from *Euplotes* species, blepharismins from *Blepharisma japonicum*, stentorins from *Stentor coeruleus* and climacostol from *Climacostomum virens* (Fig. 4).
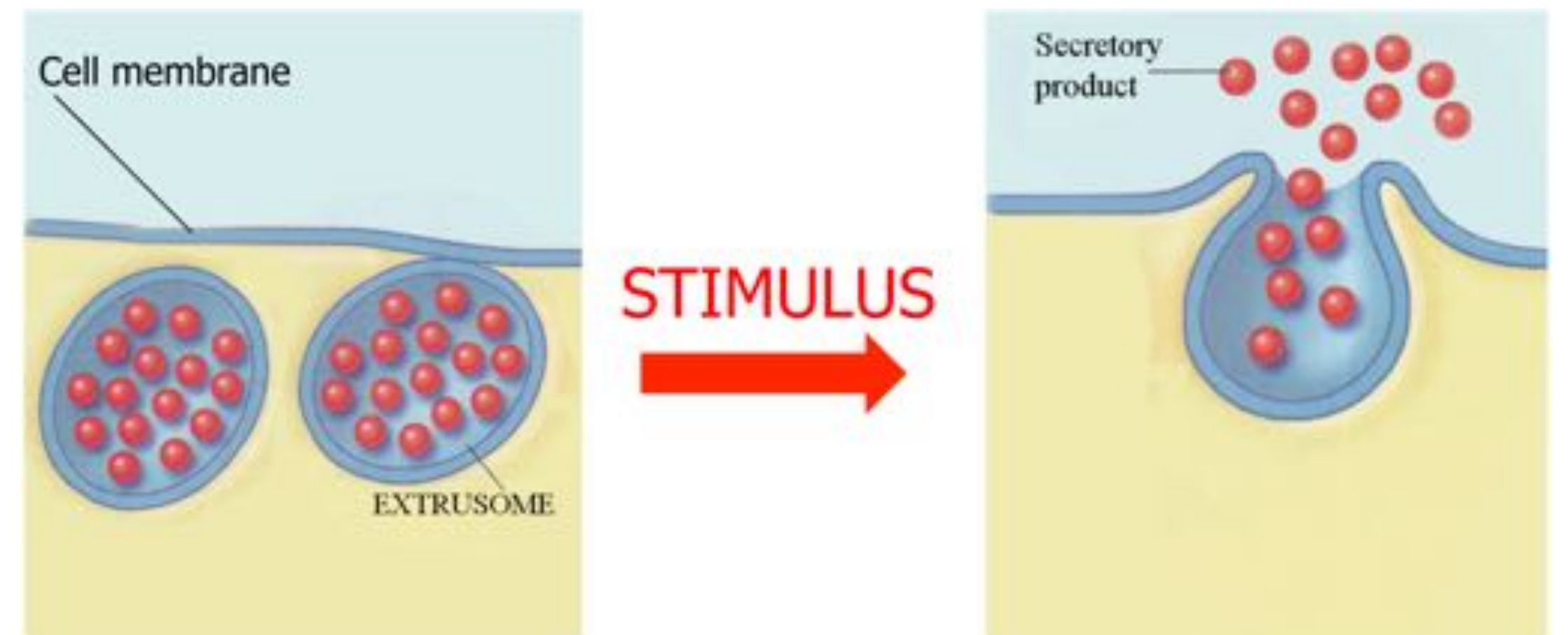
Fig.1: General mechanism of extrusome discharge.

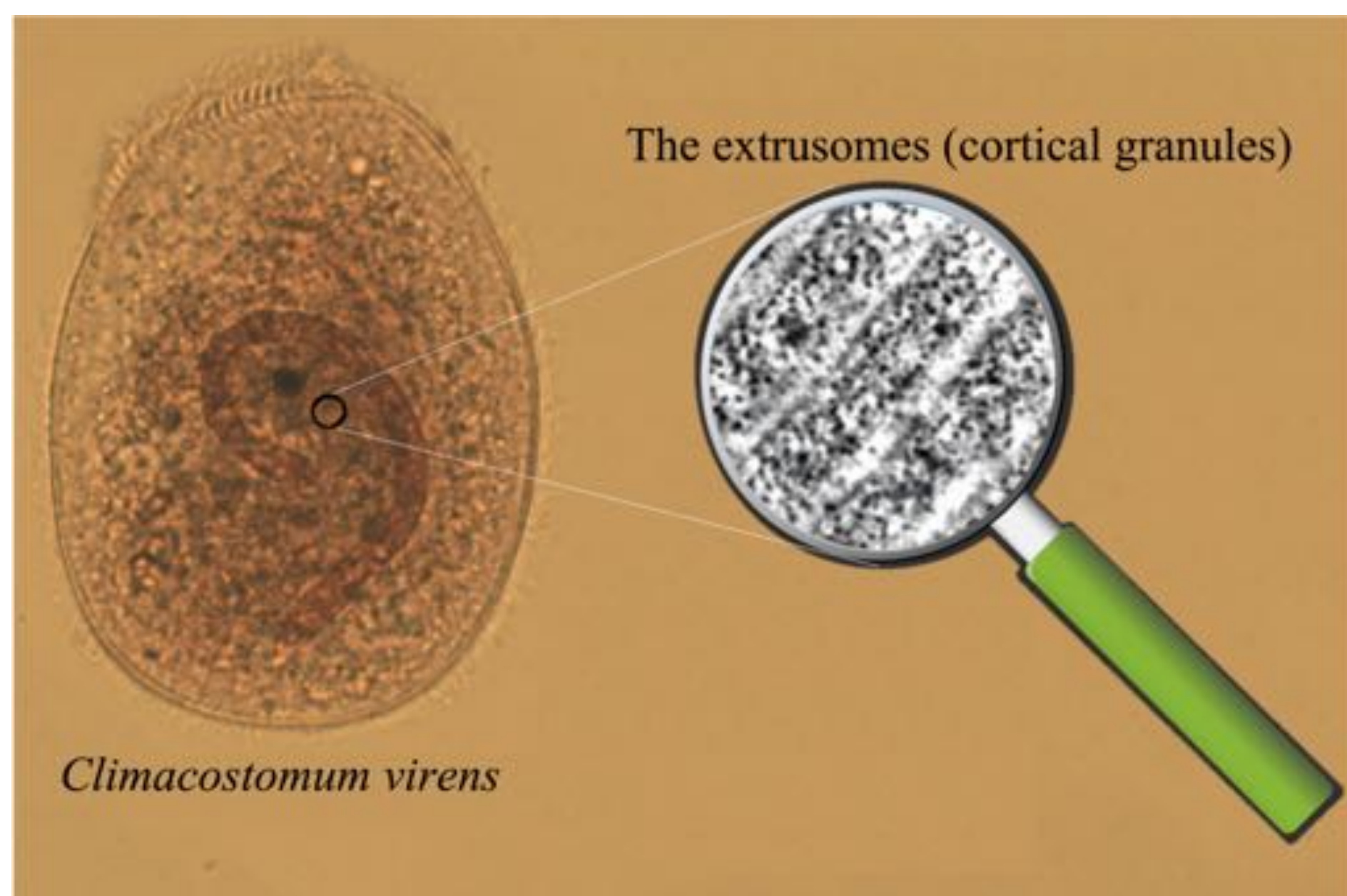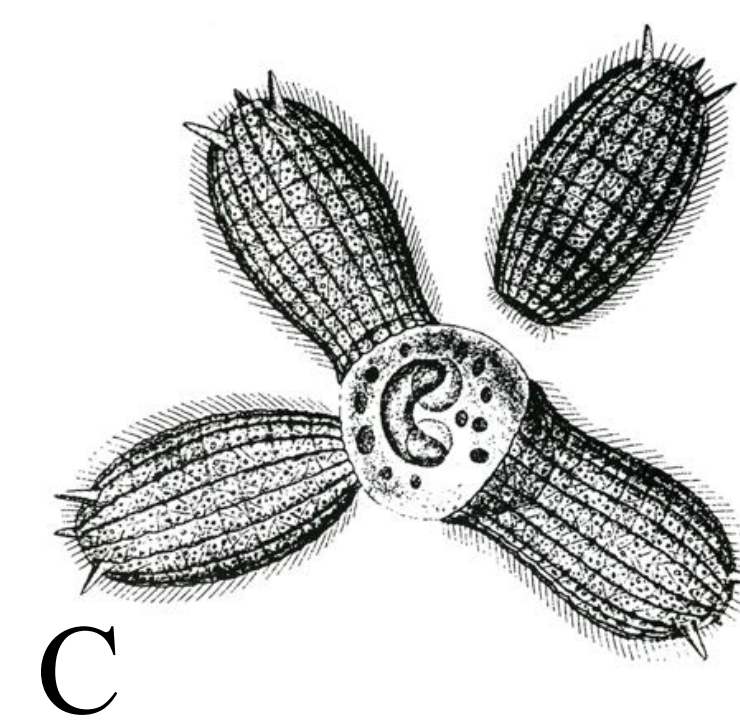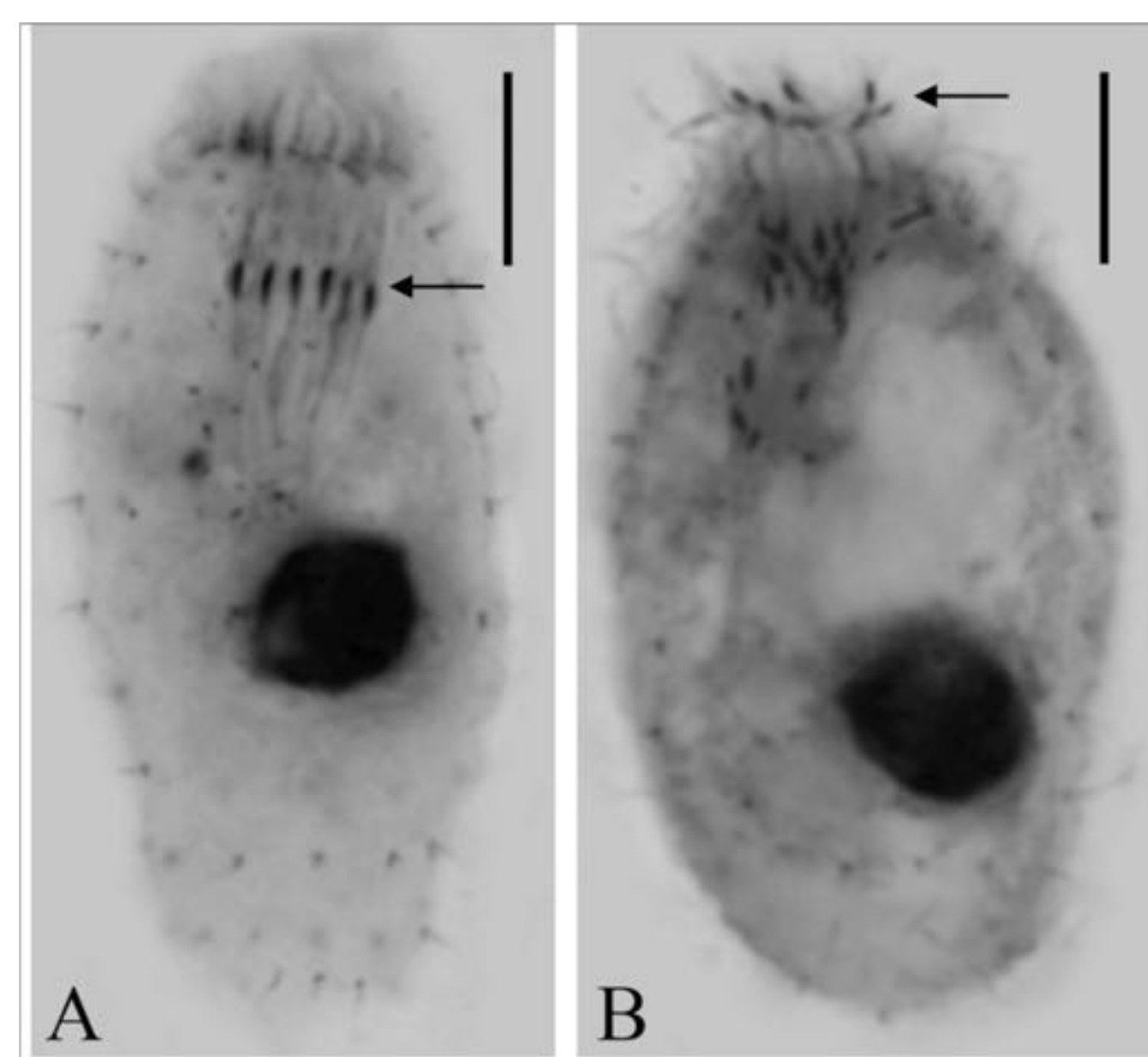Fig. 3: (A) The toxicysts of *Coleps hirtus* are visible as rod shaped organelles (arrow) in the oral basket of a cell. (B) The photomicrograph shows the toxicysts discharged (arrow) into the medium after a cold-shock treatment. Photomicrographs of fixed specimens by protargol stain, scale bar = 10 μm. (C) Predatory behavior of *C. hirtus*. (D) GC-MS-FID composition of the toxicyst discharge. Data are expressed as percentage of the total area. B = branched-chain fatty acids; C20:0 T = diterpene (phytanic acid).

Fig.2: General morphology of *Climacostomum virens* and its cortical granules visible as dots under the cell cortex.

RESULTS

Recently we have isolated the content of the toxicysts of the raptorial freshwater ciliate *C. hirtus,* and the analysis of the toxicyst discharge performed by liquid chromatography-electro-spray-mass spectrometry and gas chromatography-mass spectrometry, revealed the presence of a mixture of 19 saturated, monounsaturated and polyunsaturated free fatty acids with the addition of a minor amount of a diterpenoid, the phytanic acid. To date this is the first report for the presence of such compounds in the extrusomes of ciliated protist. In addition we have isolated and identified three new secondary metabolites contained in extrusomes (pigment granules) of the euryhialine ciliate *Pseudokeronopsis erythrina* used for chemical defense (Fig. 5). The structures of these molecules named erythrolactones A2, B2 and C2, and their respective sulfate esters (A1, B1, C1), have been elucidated on the basis of NMR spectroscopic data coupled to high resolution mass measurements (HR-MALDI-TOF), (Fig. 6). These molecules have been demonstrated to exert a toxic biological activity on a panel of free-living ciliates and microinvertebrates.
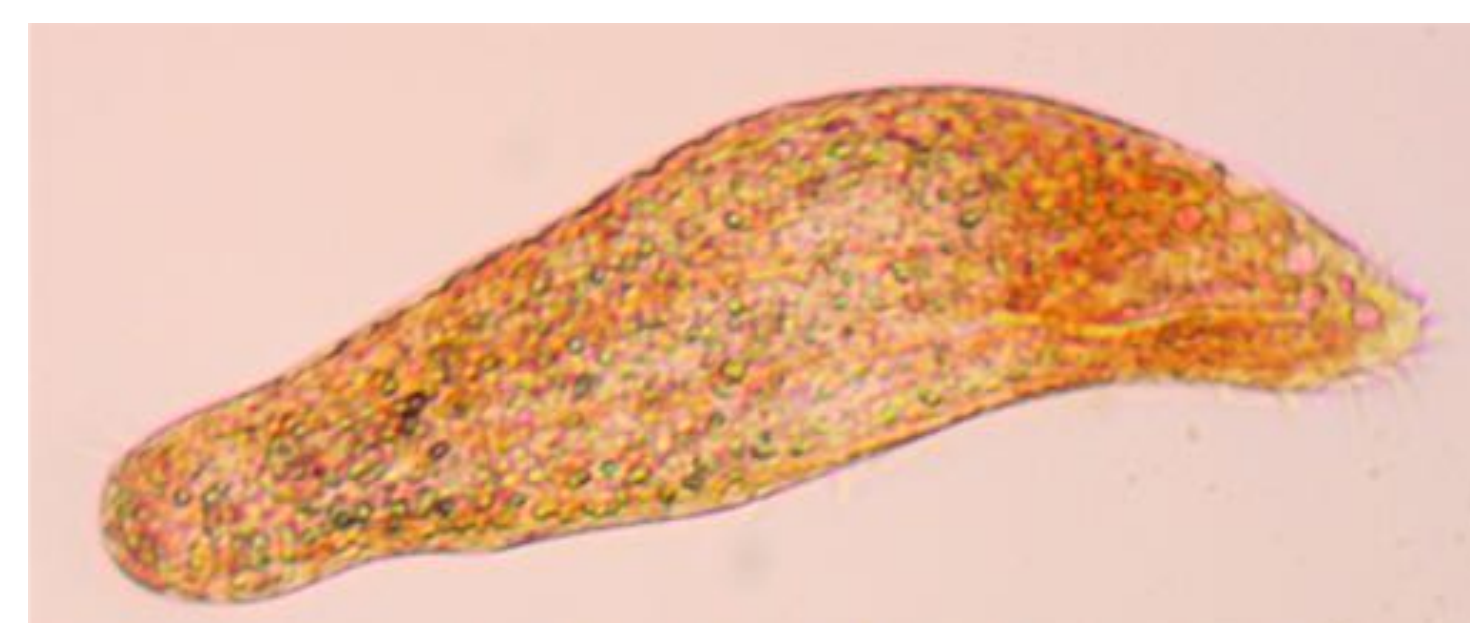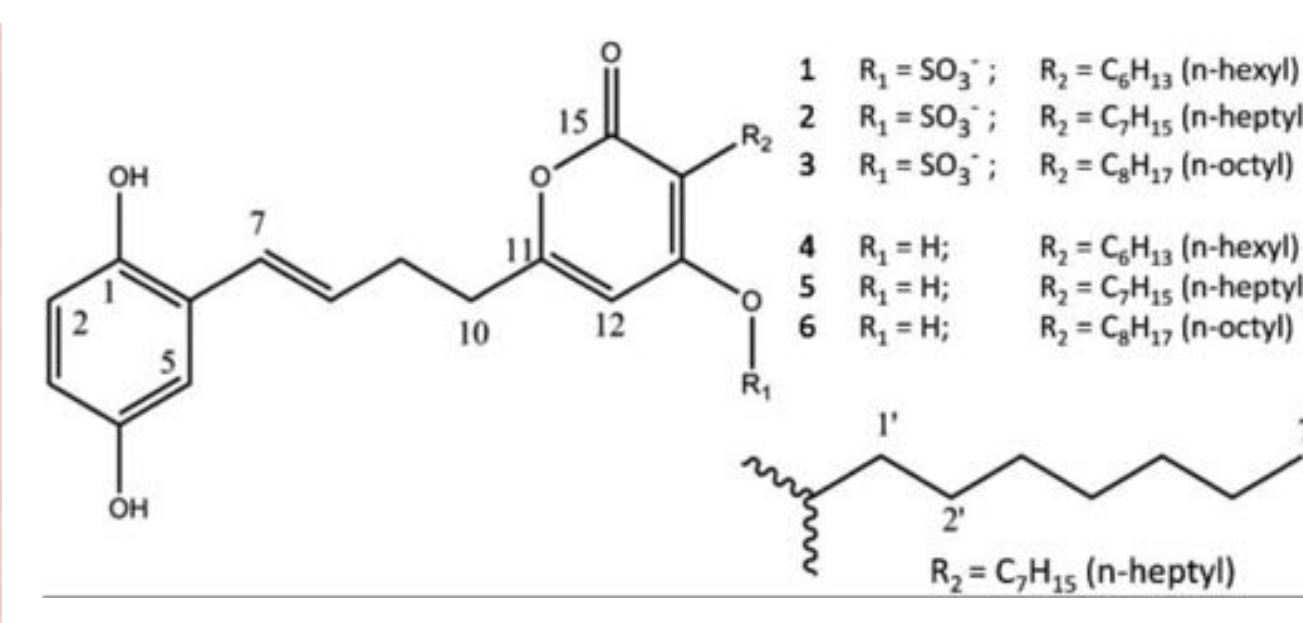
Fig. 4: Ciliates that contain identified toxic secondary metabolites for chemical defence/offence.

Fig. 5: *Pseudokeronopsis erythrina*

Fig. 6: Chemical structures of erythrolactones.

The toxin climacostol (5-(Z)-non-2-enyl-benzene-1,3-diol) isolated from *C. virens* belongs to resorcinolic lipids, a large group of natural amphiphilic compounds widely detected in prokaryotes and eukaryotes, that have attracted attention for their anti-microbial, anti-parasitic, anti-tumoral and genotoxic activities. Climacostol, now available by synthesis, displayed potent cytotoxyc activity on a panel of bacterial and fungal pathogens (Tab.1), as well as on free-living ciliated protists. This molecule is also able to inhibits the growth of tumoral cells and induces apoptosis *in vitro* (Tab.2).

Species/ Strain	climacostol	
	MIC	MBC
S. aureus		
ATCC 25923	16	16
SA019	16	16
SA040	16	16
SA047	8	8
SA070	8	16
S. epidermidis	16	32
S. pneumoniae	16	16
E. faecalis	16	16
E. coli	256	>256
P. aeruginosa	256	>256
C. albicans	8	8

Tab.1: Antimicrobial activities (MIC and MBC) of climacostol agaist a panel of representative pathogens (mg $^{L-1}$)

Cell line	Origin	Species	EC_{50}	Assay
HeLa	cervix carcinoma	human	0.605	MTT
A431	squamous carcinoma	human	~2.0	MTT/LDH
HL60	pro-myelocytic leukemia	human	~2.0	MTT/LDH
PC-3	prostatic adenocarcinoma	human	2.685	MTT
T98G	glioblastoma	human	3.545	MTT
U87MG	glioblastoma	human	4.627	MTT
P3X	myeloma	mouse	5.665	MTT
PC12	pheochromocytoma	rat	5.702	MTT
atT-20	pituitary adenoma	mouse	6.232	MTT
TM3	Leydig cells	mouse	11.30	LDH
NIH/3T3	fibroblasts	mouse	12.16	MTT
EA.hy926	endothelial cells	human	>50	MTT/LDH

Tab.2: Parameters of climacostol-induced inhibition of cell viability: tumourigenic and non-tumourigenic cell lines. EC_{50} (μg/ml) = concentration required to produce 50% of the effects. MTT or LDH assays were performed treating cells for 24 h in the absence (vehicle) or in the presence of increasing concentrations of climacostol.

In light of our definition of the *in vitro* cytotoxic activity against melanoma cells we tested the *in vivo* efficacy of climacostol. To this end B16-F10 cells were injected subcutaneously to mice; when the syngeneic implantation was established mice were injected intra-tumorally (100 μl) with vehicle (control) or climacostol at 600 μg/ml every 3-4 days for 3 weeks. Climacostol decreased tumor volumes throughout the entire study period (Fig. 7A). In particular, as shown in the tumor volume analysis of Fig. 7B, 1 tumor growth rate increased steadily for vehicle-treated animals (control) while we observed a significant and persistent inhibition of tumor load in the case of transplants treated with climacostol. In agreement with these results, the Kaplan-Meier analysis of Fig. 7C revealed that climacostol significantly improved the survival of B16-F10-injected mice (median of survival: control = 18 days, climacostol-treated group = 29 days). In separate experiments, tumors were removed at day 16 of treatment with climacostol at 600 μg/ml. As shown in Fig. 8A-B, climacostol significantly decreased tumor weight by ca. 60% when compared to vehicle-treated group (control). Consistently, climacostol exposure induced a remarkable reduction of viable cells inside the tumor (ca. 55% reduction *vs* control) (Fig. 8C). These results demonstrate that climacostol exerts an inhibitory action on melanoma progression by triggering the death process in melanoma allografts.
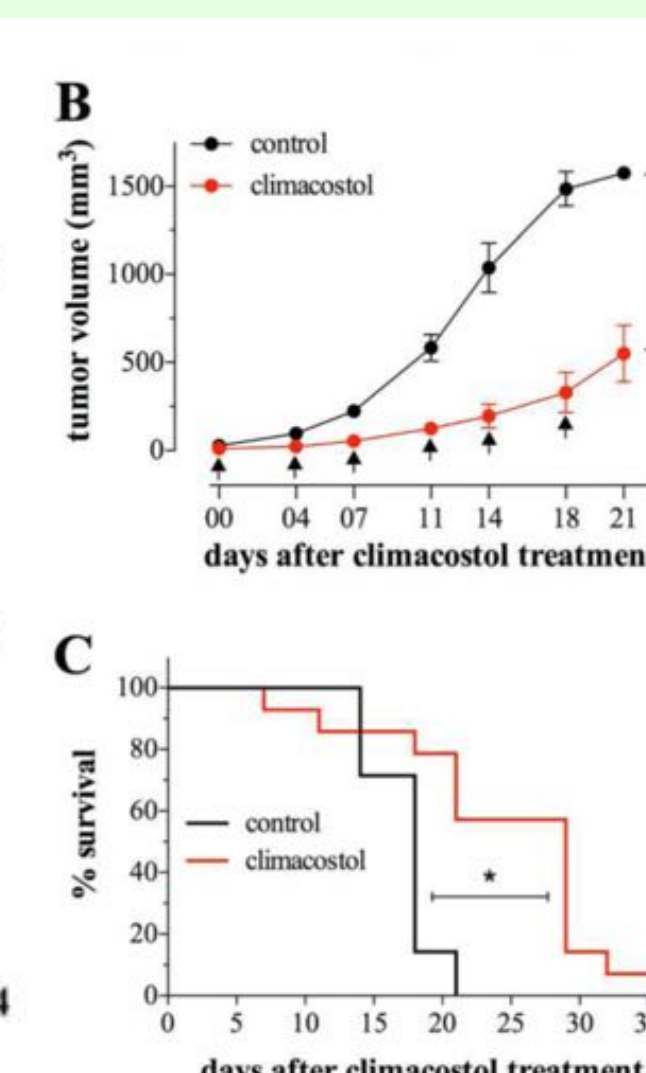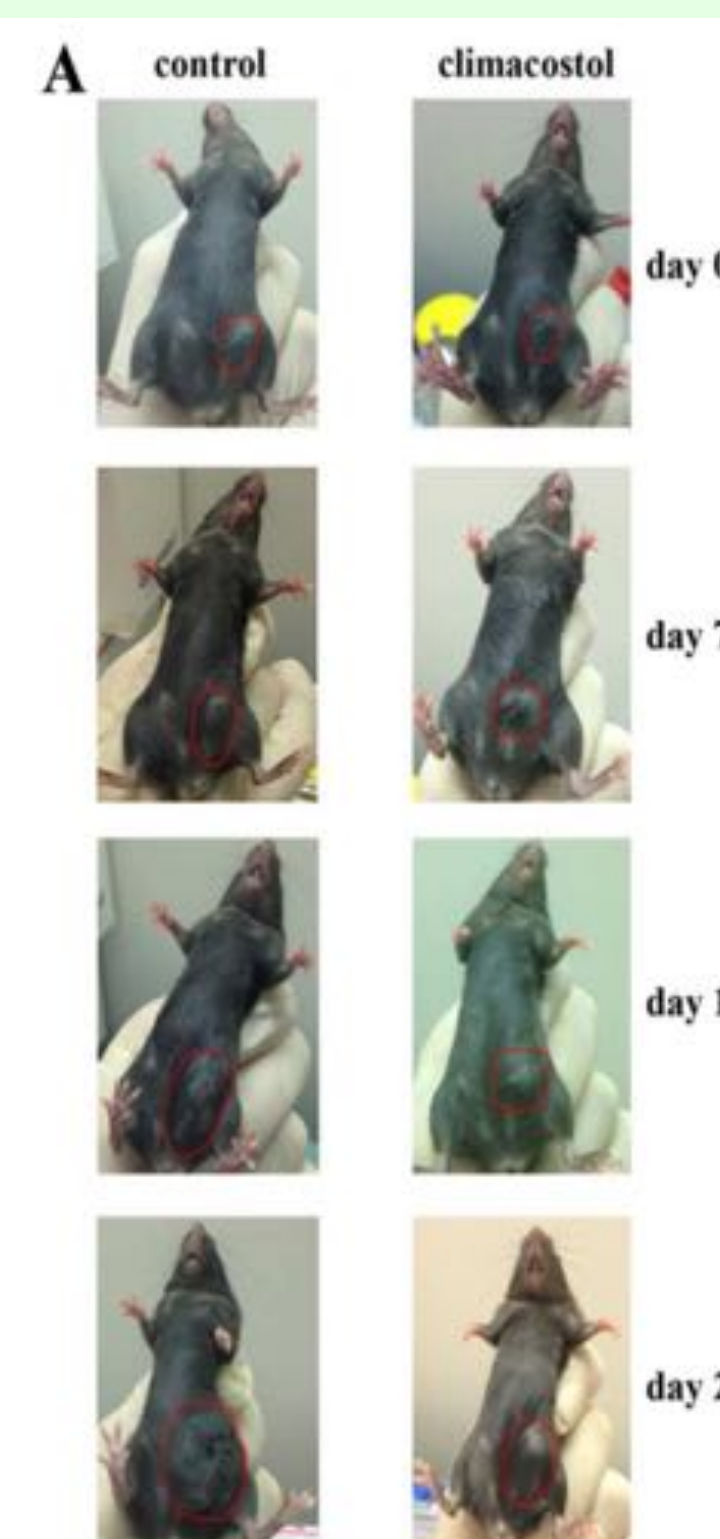
Fig.7: Anti-tumoral properties of climacostol in mice bearing B16-F10 melanoma allografts (600 μg/ml every 3-4 days for 3 weeks or vehicle) (B) Tumor growth. (C) Percentage survival analyzed by Kaplan-Meier curve (7-15 animals per experimental group.*p<0.001 *vs* control).
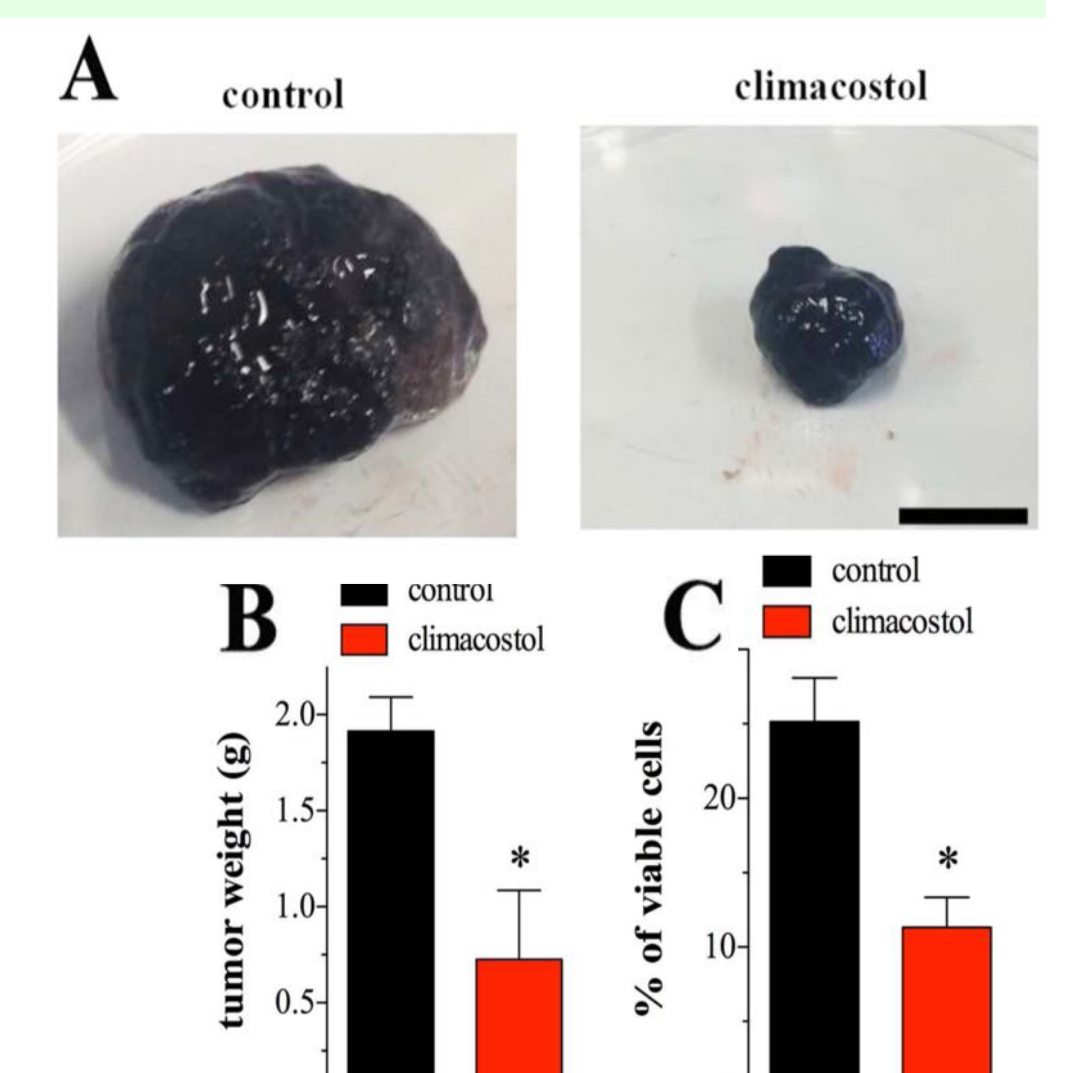
Fig.8: Subcutaneous melanoma allografts 1 excised from mice at day 1 of treatment (from day 0 - every 3-4 days) with vehicle (control) or climacostol (600 μg/ml). Scale bar: 5 mm. (B) Weight of the excised tumors. (C) Percentage of viable cells inside the tumors. Results obtained from 3 animals per experimental group.*p<0.05 *vs* control.